The Impact of High-Temperature Superconductivity on SQUID Magnetometers

JOHN CLARKE AND ROGER H. KOCH

DC and RF Superconducting QUantum Interference Devices (SQUIDs) fabricated from low transition temperature (T_c) superconductors and operated at liquid ^{4}He temperatures are routinely used as ultrasensitive detectors in many applications, for example, as magnetometers, magnetic gradiometers, voltmeters, and motion detectors. SQUIDs fabricated from high T_c superconductors such as $YBa_2Cu_3O_7$ and operated in liquid nitrogen at 77 K offer a greater convenience in operation at the expense of a poorer noise performance, particularly at low frequencies. The resolution of SQUID-based magnetometers is compared with that of other types of magnetometers operating at ambient temperatures.

WHAT WILL BE THE IMPACT OF HIGH-TEMPERATURE superconductivity on Superconducting QUantum Interference Devices (*1*) (SQUIDs)? Besides being the most sensitive magnetometer available, the SQUID has been used in many other applications, for example as a voltmeter, amplifier, motion detector, and susceptometer. SQUIDs have been by far the most widely used superconducting device and are likely to be the first practical application of the new oxide superconductors. By combining the phenomena of fluxoid quantization (*2*) and Josephson tunneling (*3*), SQUIDs convert changes in magnetic field into voltages that can be detected by conventional semiconducting electronics. Until very recently these devices involved superconducting metals such as niobium or lead and their alloys and were almost invariably operated at or below the boiling point of liquid ^{4}He under atmospheric pressure, 4.2 K. Thus, in choosing a magnetometer one had to weigh the advantages of a very sensitive device operating in liquid ^{4}He against those of a less sensitive magnetometer operating at room temperature. In some applications, such as the detection of tiny magnetic signals emanating from the human brain, only SQUID-based instruments have the required sensitivity, and they are invariably used. In other applications, such as geophysical measurements, which are often made in remote areas of the world, the inconvenience of using liquid helium often outweighs the advantage of very high sensitivity, and alternative instruments, such as coil magnetometers, are much more widely used.

This situation may be about to change dramatically, however, with the advent of high-temperature superconductivity (*4*). Materials such as $YBa_2Cu_3O_{7-\delta}$ (YBCO) (*5*) with a superconducting transition temperature (T_c) of about 95 K and the recently discovered compounds involving Bi-Sr-Ca-Cu-O (*6*) and Tl-Ca-Ba-Cu-O (*7*) with transition temperatures of 110 K and 125 K, respectively, offer the possibility of operating SQUIDs at the boiling point of liquid N_2, 77 K. Indeed, several groups have already demonstrated SQUIDs operating at or close to this temperature. But one pays a price for higher temperature operation—the resolution will inevitably degrade as the temperature is raised. Again one will be forced to make choices: Is the loss in performance justified by the greater ease of operation in liquid N_2? Are SQUIDs at 77 K still more sensitive than competing magnetometers operating at room temperature? Not surprisingly, the answers depend on numerous factors, for example, the frequency range, whether the magnetometer is in a well-equipped facility or in a remote area, the time over which one would like to operate the magnetometer unattended and, of course, the exact nature of the measurement. In this article we attempt to address these issues.

Superconductivity, Flux Quantization, and SQUIDs

The central feature of both low T_c and high T_c superconductors is the formation of Cooper pairs of electrons or holes. Cooper pairs can carry a current, namely a supercurrent, without the Joule heating generated in a normal conductor. They are also involved in the phenomenon of fluxoid quantization (*2*): the magnetic flux thread-

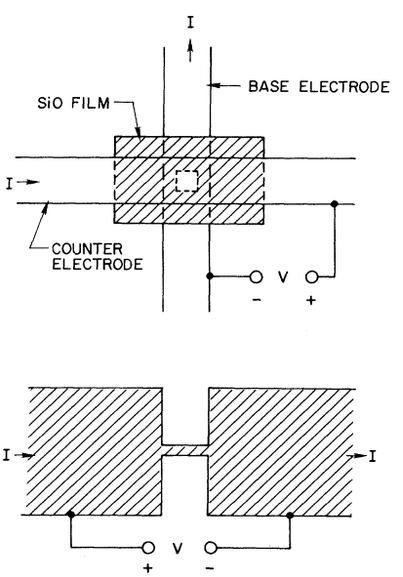

Fig. 1. (**Top**) Thin-film Josephson tunnel junction fabricated from low T_c superconductors. The base electrode, usually Nb, is oxidized or covered with a thin layer of Al_2O_3, and a counter electrode, usually Nb or a Pb alloy, is deposited to complete the junction. The area of the junction is defined by the window in the SiO film. (**Bottom**) Anderson-Dayem bridge, consisting of a superconducting film necked down to produce a weak link with a small cross section.

J. Clarke is at the Department of Physics, University of California, and the Center for Advanced Materials, Materials and Chemical Sciences Division, Lawrence Berkeley Laboratory, Berkeley, CA 94720. R. H. Koch is at the IBM Research Division, Thomas J. Watson Research Center, Yorktown Heights, NY 10598.

ing a thick, superconducting ring is equal to $n\Phi_0$, where n is an integer and $\Phi_0 \equiv h/2e \approx 2 \times 10^{-15}$ Wb is the flux quantum (1 Wb = 10^8 gauss-cm^2). If one applies a flux of arbitrary value Φ to a ring of inductance L, flux quantization causes the ring to generate a supercurrent $J = -\Phi/L$, so that the self-generated flux $LJ = -\Phi$ exactly cancels Φ. A third attribute of Cooper pairs is Josephson tunneling (*3*). A Josephson tunnel junction (Fig. 1, top) consists of two superconducting thin films, for example Nb, separated by a thin (~2 nm) insulating layer. When one passes a current I through the junction the Cooper pairs tunnel quantum mechanically through the barrier, and no voltage V is developed until I exceeds a maximum value, the critical current I_0. For use in SQUIDs, the junctions are usually shunted with a resistance R. This resistance eliminates hysteresis in the I-V characteristic provided $\beta_c \equiv 2\pi I_0 R^2 C/\Phi_0 \lesssim 1/2$, where C is the self-capacitance of the junction (*8, 9*). Figure 1, bottom, shows a different kind of "weak link," the Anderson-Dayem bridge (*10*). The bridge is intrinsically superconducting, with a sufficiently small cross section that it can sustain only a very small supercurrent. The bridge exhibits Josephson-like behavior provided its length is no greater than the coherence length ξ, which is, roughly speaking, the spatial extent of a Cooper pair. In materials such as Nb or Pb, $\xi \approx 100$ nm, a dimension that can be readily achieved with today's lithographic techniques.

Although the technology for making junctions from low T_c superconductors, such as niobium, is extremely well developed, there is not yet a comparable process for making tunnel junctions from high T_c superconductors, which invariably require high-temperature processing. YBCO has been formed into structures similar to that in Fig. 1, bottom, but the length of bridge is much greater than ξ, which is estimated to be rather less than (somewhat greater than) 1 nm for directions perpendicular to (parallel to) the crystalline planes. The critical current is determined by one or more grain boundaries crossing the bridge (*11, 12*) so that the behavior is probably closer to that of a Josephson junction than that of an Anderson-Dayem bridge.

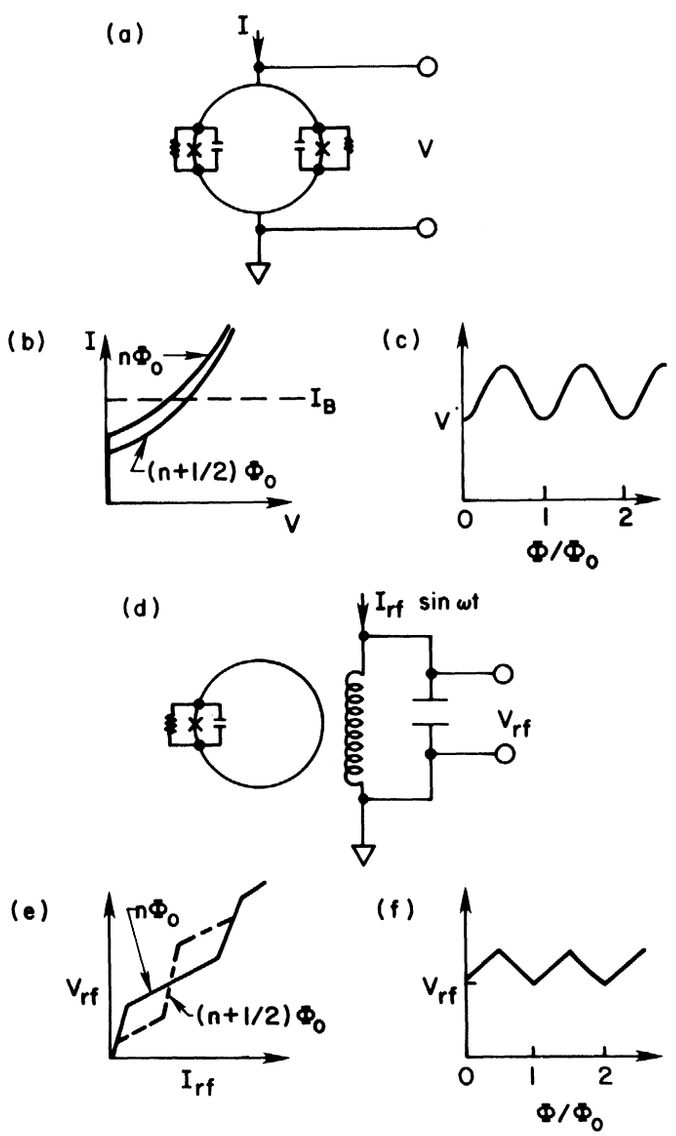

Fig. 2. (**a**) Schematic representation of dc SQUID; (**b**) I-V characteristics for $\Phi = n\Phi_0$ and $(n + 1/2)\Phi_0$; (**c**) V versus Φ for constant current bias; (**d**) schematic representation of rf SQUID; (**e**) peak amplitudes of V_{rf} versus I_{rf} for $\Phi = n\Phi_0$ and $(n + 1/2)\Phi_0$; (**f**) peak amplitude of V_{rf} versus for fixed I_{rf}.

DC SQUIDs

The two types of SQUIDs are shown schematically in Fig. 2. The dc SQUID (*13*) consists of two Josephson junctions interrupting a superconducting ring of inductance L. The prefix "dc" implies that the device is biased with a direct current. The total critical current of the two junctions is periodic in the external flux passing through the ring, with a period Φ_0. This behavior is similar to the fringe pattern observed when two coherent beams of light interfere—hence the name "Superconducting QUantum Interference Device." As we see in Fig. 2b, the voltage across the SQUID depends on both the bias current and the applied magnetic flux. Because the devices are normally operated by fixing the bias current at a constant value and measuring the change in voltage that occurs for a small change in applied flux (Fig. 2c), the SQUID is a flux-to-voltage converter.

Although the periodic behavior is an elegant manifestation of the quantum nature of superconductivity, in practice one usually requires the output voltage to be proportional to the input flux even when the applied flux is much greater than Φ_0. This linear response is obtained by means of a feedback circuit in which the SQUID acts as a null-flux detector. A flux change $\delta\Phi$ produces a voltage across the SQUID that is amplified by room-temperature electronics and converted into a current through a coil coupled to the SQUID, thereby generating a flux $-\delta\Phi$. In this way, we cannot only detect a flux $\delta\Phi$ much less than Φ_0, but also measure an applied flux corresponding to many Φ_0. To minimize drift and low-frequency noise, in practice one applies an alternating flux to the SQUID, and amplifies the resulting alternating voltage. A typical system (*14*) has a dynamic range of $\pm 2 \times 10^7$ Hz$^{-1/2}$ for signal frequencies below 6 kHz, a frequency response (±3 dB) from 0 to 70 kHz, and a maximum slew rate (at 6 kHz) of 3×10^6 Φ_0 s^{-1}.

The most sensitive dc SQUIDs involve thin films patterned with photo or electron-beam lithography. A successful and widely used design is that of Ketchen and Jaycox (*15*), one version of which is shown in Fig. 3, top left. Following a normal film that forms the resistive shunt for each junction, one deposits a square "washer" of Nb containing a slit to form most of the SQUID loop, and then patterns an insulating layer (usually SiO). Two tunnel barriers are formed on the Nb exposed through the two windows defining the junctions (Fig. 3, bottom) either by growing an insulating layer of native oxide or by oxidizing a deposited film of Al (*16*). The SQUID is completed with the deposition of a superconducting counterelectrode that connects the junctions. An input coil, consisting of a spiral of Nb film, is deposited over the washer to provide tight magnetic coupling to the SQUID. The pads at the ends of the spiral coil provide connection to an appropriate circuit, for example, the

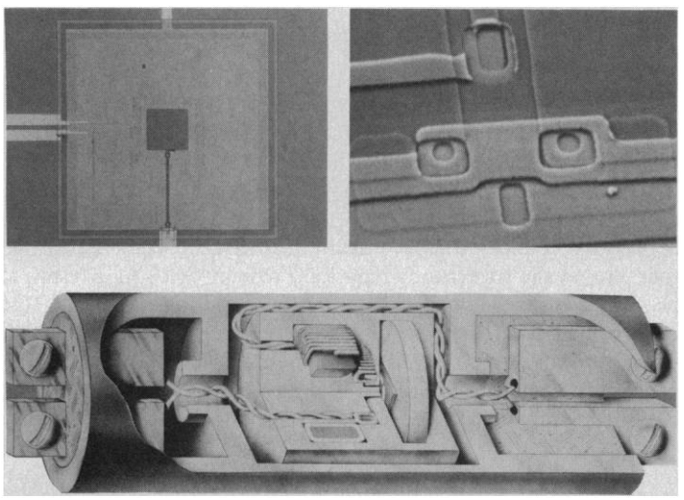

Fig. 3. (**Top left**) Planar dc SQUID made with niobium technology. A four-turn spiral coil overlays the SQUID. The region shown in the image is 1.3 mm wide and 1 mm high. (**Top right**) Window junctions in the device before deposition of counter electrode. The region shown is 34 μm wide and 26 μm high. (**Bottom**) Toroidal rf SQUID. The SQUID is 4 cm long.

magnetometer to be discussed below.

The sensitivity of a SQUID is determined by the voltage noise it generates in the absence of a signal. This voltage noise can be expressed as an equivalent magnetic-flux noise with a power spectral density (mean square flux per unit bandwidth) $S_\Phi(f)$ at frequency f. Typically, $S_\Phi(f)$ is white or frequency independent down to low frequencies where it scales approximately as $1/f$. There is a well-established theory (*17*) for the white noise, which originates from the Nyquist noise in the resistive shunts. A useful figure of merit for comparing different SQUIDs is the flux noise energy per unit bandwidth $\varepsilon(f) \equiv S_\Phi(f)/2L$. For an optimized SQUID, with $\beta \equiv 2LI_0/\Phi_0 = 1$, the white noise energy is found to be

$$\varepsilon(f) \simeq 9k_BTL/R \qquad (1)$$

For a SQUID involving tunnel junctions, setting $\beta_c = 1/2$ we find

$$\varepsilon(f) \simeq 25k_BT(LC)^{1/2} \qquad (2)$$

Equation 2 indicates that ε increases with T and with L and C. A large variety of SQUIDs have noise energies in good agreement with Eq. 2. In particular, SQUIDs like that in Fig. 3, top left, with inductances of 100 to 500 pH have typical noise energies of (1 to 5) $\times 10^{-32}$ J/Hz $\approx 100\hbar$ to $500\hbar$; a typical value is shown in Fig. 4. We note in passing that when L, C, and T are reduced sufficiently the noise energy is predicted to be limited by quantum mechanical effects to a value of order $\hbar$; for this reason, noise energies are often quoted in units of $\hbar$ (*18*).

The $1/f$ noise is much less predictable and arises from at least two mechanisms. The first is fluctuations in the critical current, I_0, of the Josephson junctions. Electrons captured or released from trapping sites in the insulating barrier cause local fluctuations (*19*) in the tunnel barrier potential energy and hence in the exact value of I_0. Each trap has an associated trapping time τ and produces a Lorentzian power spectrum of the form $[1 + (2\pi f\tau)^2]^{-1}$. The sum of a number of Lorentzian spectra with a distribution of τ's yields a power spectrum scaling as $1/f$ (*20*). Poor quality junctions with many traps tend to have high levels of $1/f$ noise, whereas high-quality junctions having relatively few traps have correspondingly low noise levels and sometimes the individual Lorentzians are clearly visible. The trapping and detrapping processes are generally thermally activated (except, perhaps, at very low temperatures) so that the level of $1/f$ noise increases rapidly with temperature. Fortunately, the magnitude of the critical current noise can be considerably reduced by techniques involving double modulation of the SQUID (*21–23*).

The second source of $1/f$ noise is less well understood, manifesting itself as an apparent flux noise (*22*). It is believed that the noise is produced by flux quanta that are thermally activated from one pinning site to another in the body of the SQUID. The magnitude of this noise varies considerably with the composition and microstructure of the film forming the SQUID body. In typical Nb-based devices the spectral density of the noise is about 10^{-10} Φ_0^2/Hz, at 1 Hz (Fig. 4) but other SQUIDs have exhibited substantially lower values (*23–25*). The lowest reported value (*23*) of $1/f$ noise power, 10^{-10} Φ_0^2/Hz, at 10^{-2} Hz was obtained with high-quality Nb films with the aid of a double modulation scheme to reduce the $1/f$ noise caused by critical current fluctuations. It is important to realize that $1/f$ flux noise cannot be reduced by any known modulation scheme.

RF SQUIDs

The rf SQUID (Fig. 2d) consists of a superconducting loop interrupted by a single Josephson junction (*26*). The prefix "rf" implies the device is biased with a radio-frequency flux. The loop is coupled to the inductance of a tuned tank circuit driven with a current at its resonant frequency, typically $\omega_{rf}/2\pi = 20$ MHz. Figure 2e shows the peak amplitude of the voltage, V_{rf}, across the tank circuit versus the peak amplitude of the current I_{rf}. For $\Phi = n\Phi_0$, the characteristic consists of a set of steps and risers. As Φ is increased to $(n + 1/2)\Phi_0$ the steps split. At a suitable value of I_{rf}, the voltage V_{rf} is periodic in Φ_0 as shown in Fig. 2f. Thus, one can

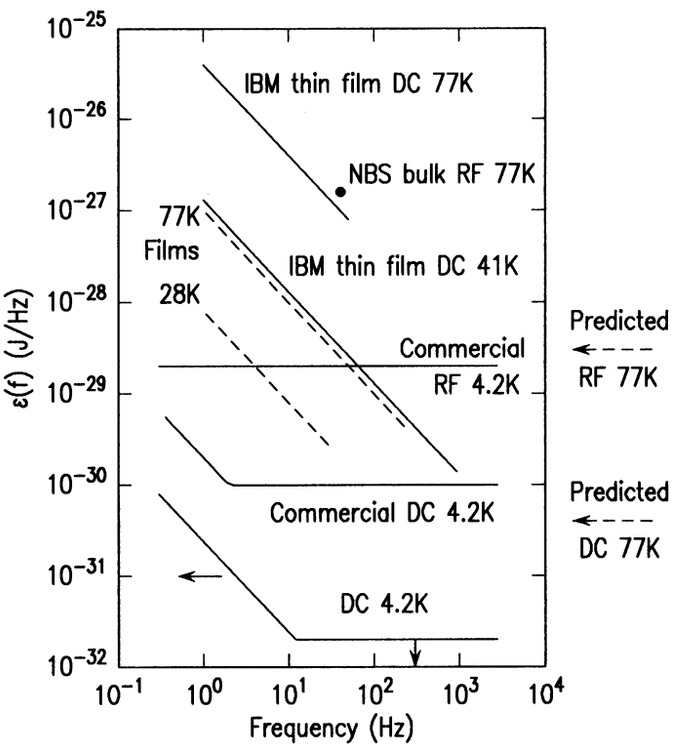

Fig. 4. Noise energies of various SQUIDs (solid lines). The white noise predicted for dc and rf SQUIDs (dashed arrows) and the noise in a YBCO loop at 77 K and 28 K are also plotted (dashed lines). Lower white- and $1/f$-noise levels have both been achieved at 4.2 K with dc SQUIDs (indicated by arrows).

operate the rf SQUID in a flux-locked loop in the same way as the dc SQUID.

Because the dc SQUID is the more sensitive device, there has been little development of the rf SQUID for more than a decade. The most widely used version has a toroidal body machined from Nb and contains a thin-film Nb junction (Fig. 3, bottom) (*21*). (A dc SQUID is available in a similar configuration.) Flux is coupled to the SQUID by means of a toroidal coil of Nb wire. Typically, the slew rate and dynamic range are comparable with those of the dc SQUID. In one commercially available system (*27*), one obtains a large dynamic range ($>10^9/\text{Hz}^{1/2}$) by allowing the feedback system to reset each time an additional flux quantum is applied to the SQUID: the output signal represents the input flux in the form $(n + \delta n)\Phi_0$, where $\delta n < 1$. Despite its lower sensitivity compared with its two-junction counterpart, the rf SQUID is adequate for many applications, and the absence of any direct electrical connection reduces the risk of accidental junction burnout by massive extraneous pulses.

The theory for white noise in the rf SQUID is well developed, but complicated by the fact that for 4.2 K operation the contributions of the preamplifier and the tank circuit are not negligible as they usually are for the dc SQUID. Because the tank-circuit capacitance is partly at room temperature, the effective noise temperature of the tank circuit is generally much higher than the bath temperature. The intrinsic SQUID noise energy for $LI_0 = \Phi_0$ is predicted to be (*28, 29*)

$$\varepsilon(f) \simeq (LI_0^2/\omega_{rf})(2\pi k_B T/I_0\Phi_0)^{4/3} \quad (3)$$

If we take as reasonable values $\omega_{rf}/2\pi = 20$ MHz and $I_0 = 5$ μA, at 4.2 K we find 10^{-30} J/Hz. Measured performance, however, is substantially poorer: a typical value is $\varepsilon \approx 5 \times 10^{-29}$ J/Hz, implying that extrinsic noise sources dominate (see Fig. 4). The $1/f$ noise also appears to be higher than for dc SQUIDs, with a typical value of 10^{-29} J/Hz at 1 Hz.

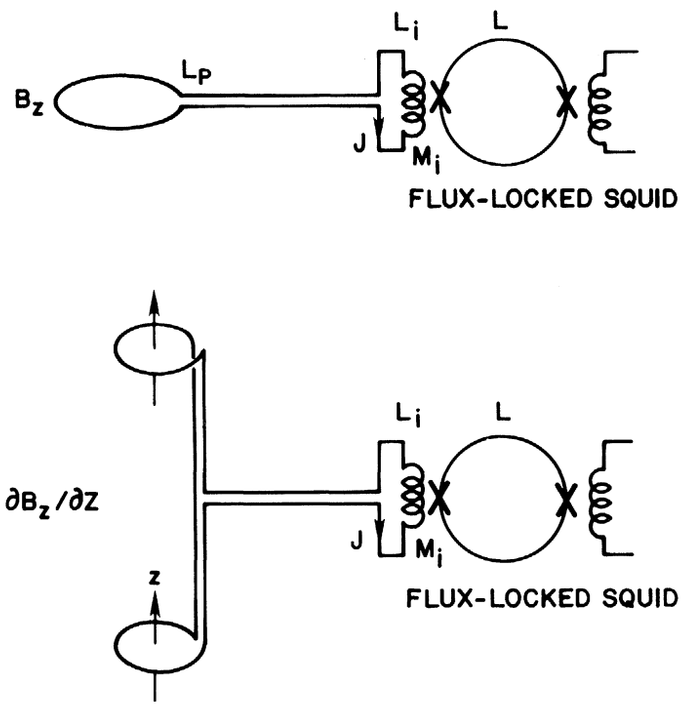

Fig. 5. Superconducting flux transformers to measure (**top**) magnetic field, B_z, and (**bottom**) magnetic field gradient $\partial B_z/\partial z$. In each case the transformer consists of a continuous length of niobium wire connected to the input coil of a SQUID. The SQUID and its input-coil are surrounded by a superconducting shield to exclude magnetic field changes.

Flux Transformers, Magnetometers, and Gradiometers

SQUIDs themselves are not necessarily highly sensitive detectors of magnetic field; indeed, the toroidal configuration of Fig. 3, bottom, is impervious to external fields. Virtually all magnetometers involve the use of superconducting loops or wires to form a flux transformer as shown in Fig. 5, top. When a magnetic field is applied to the pick-up loop, fluxoid quantization requires that the total flux in the superconducting loop remain fixed. As a result, a persistent supercurrent is generated, producing flux in the SQUID. A simplified analysis shows that optimum sensitivity is obtained when the inductances of the pick-up loop, L_p, and input coil, L_i, are equal. For a single-turn pick-up loop of radius r_p, the noise in the SQUID is equivalent to a magnetic field noise (*30*)

$$B_N(f) \simeq (2\sqrt{2}\, L_p^{1/2}/\pi r_p^2)[\varepsilon(f)/\alpha^2]^{1/2} \quad (4)$$

where α^2 is the coupling coefficient between the SQUID and the input coil. Since L_p is approximately proportional to r_p, Eq. 4 implies that the sensitivity to magnetic field scales as $r_p^{-3/2}$, that is, that the sensitivity can in principle be improved indefinitely if one makes the pick-up coil large enough. In practice, of course, the constraint $L_p = L_i$, the size of the cryostat and noise generated within the cryostat all impose practical limitations. As an example, for geophysical applications a reasonable magnetic field resolution is 10^{-14} T/Hz$^{1/2}$ (1 tesla = 10^4 gauss = 10^9 gamma). This value is not hard to achieve: for a toroidal rf SQUID with the somewhat conservative parameters $\varepsilon = 10^{-28}$ J/Hz and $\alpha^2 = 0.5$, we find $r_p = 25$ mm (*31*). With the higher resolution of the dc SQUID, the loop can be correspondingly smaller: Wellstood *et al.* (*25*) made a thin-film SQUID with an integrated thin-film pick-up loop a few millimeters across and achieved a white noise of 5×10^{-15} T/Hz$^{1/2}$.

An important extension of the flux transformer is to the measurement of magnetic field gradients, notably for neuromagnetism (*32*), a rapidly growing field in which one measures minute magnetic signals, as low as 10^{-13} T, emanating from the electrical currents in neurons in the human brain. These signals must be measured in the presence of both man-made and natural magnetic field noise that can be as high as 10^{-9} T/Hz$^{1/2}$ at 1 Hz. An elegant way of rejecting the ambient interference in favor of the locally generated signal is by means of a gradiometer. A magnetometer (Fig. 5, top) measures the magnitude of a magnetic field in a given direction, whereas a gradiometer measures the spatial derivative of the field. Figure 5, bottom, shows a first-derivative gradiometer ($\partial B_z/\partial z$) consisting of two matched pick-up loops wound in opposition to each other and connected in series with the input coil of the SQUID. A uniform magnetic field B_z generates equal and opposite fluxes in the transformer producing no input to the SQUID, whereas a gradient $\partial B_z/\partial z$ links a net flux to the transformer, producing a signal in the SQUID. Because gradients from a magnetic dipole fall off as $1/r^4$, the gradiometer discriminates against magnetic interference from distant sources in favor of locally generated signals. To provide even higher noise rejection, second-derivative gradiometers ($\partial^2 B_z/\partial z^2$) are often used. To reduce magnetic field fluctuations even further, it is becoming common practice to place the instrument and patient in a shielded room consisting of multiple layers of mu-metal and aluminum. With appropriate design of the liquid helium dewar, one can bring one end of the gradiometer operating at 4.2 K to within 10 mm or less of the subject's scalp. The distance to the brain may be comparable with the baseline of the gradiometer, so that the instrument largely measures the magnetic field, rather than its derivative. Typically sensitivities are about 2×10^{-14} T/Hz$^{1/2}$. Under favorable circumstances an array of such devices enables one

to locate the source of the magnetic field to within a few millimeters; the source might involve the collective firing of typically 10,000 neurons.

In recent years, a number of workers (*33–35*) have built integrated gradiometers in which thin-film pick-up loops are deposited on the same chip as a thin-film SQUID. Because the structure is confined to two dimensions, gradiometers of this kind measure off-diagonal gradients, for example, $\partial B_z/\partial x$ or $\partial^2 B_z/\partial x \partial y$. To obtain improved spatial resolution and greater data acquisition rates in biomagnetic measurements, a large array of gradiometers (say 100 or more) would be most advantageous and future developments are likely to involve thin-film devices.

High T_c SQUIDs

We now turn to the impact of high-temperature superconductivity on SQUIDs. Although the effect of new materials operating at much higher temperatures on the $1/f$ noise is impossible to predict, we can make reasonable estimates of the white-noise levels potentially achievable.

Thermal noise imposes two constraints on SQUID parameters. For quantum effects to be observable, the root-mean-square flux noise in the loop, $(k_B TL)^{1/2}$, should be less than $\Phi_0/4$. Computer simulations yield a similar restriction. At 77 K we find $L < 1$ nH, a requirement actually satisfied by most SQUIDs operated at 4.2 K. In addition, the coupling energy of each junction, $I_0\Phi_0/2\pi$, must be much greater than $k_B T$, by a factor of at least 5 according to computer simulations; this implies $I_0 > 16$ μA at 77 K. If we take as arbitrary but reasonable values of $L = 0.2$ nH and $I_0 = 20$ μA, we obtain $2LI_0/\Phi_0 = 4$ for the dc SQUID and $LI_0/\Phi_0 = 2$ for the rf SQUID. These values of LI_0 are quite close to optimum, and to a first approximation we can use Eqs. 1, 2, and 3 to predict the noise energies. It is somewhat unrealistic to use Eq. 2 for the dc SQUID, because tunnel junctions have not yet been made with high-T_c materials. The value of R to be used in Eq. 1 is an open question, and we adopt a value of 5 Ω, which is comparable with that used for Nb-based SQUIDs, and not too far removed from values achieved experimentally for high T_c grain-boundary junctions. With $L = 0.2$ nH, $T = 77$ K and $R = 5$ Ω, Eq. 1 yields a predicted value of $\varepsilon \approx 4 \times 10^{-31}$ J/Hz. This noise energy is only one order of magnitude higher than that measured in thin-film SQUIDs at 4.2 K, and actually slightly better than that of commercially available toroidal SQUIDs. If one could achieve this performance in a 77 K SQUID at frequencies down to 1 Hz or less, it would be adequate for the majority of SQUID applications.

For the rf SQUID, with $\omega_{rf}/2\pi = 20$ MHz and $T = 77$ K, Eq. 3 yields 3×10^{-29} J/Hz. This intrinsic noise energy is comparable with the overall value obtained experimentally with 4.2 K devices. Since the extrinsic or preamplifier noise sources should not increase when the SQUID temperature is raised to 77 K, it seems likely that the white noise of rf SQUIDs at liquid N_2 temperatures will be comparable with that at liquid ^{4}He temperatures.

Although a number of dc and rf SQUIDs have been made from YBCO, we will briefly describe just one of each type in which the noise has been measured. To the best of our knowledge, Koch *et al.* (*11*) were the first to make a thin-film device with YBCO, a dc SQUID. In the early devices, the films were patterned by covering the regions of YBCO to remain superconducting with a gold film and ion implanting the unprotected regions so that they became insulating at low temperatures. Figure 6, top, shows such a device before the protective gold layer has been removed. The inductance is estimated to be 80 *p*H. The two microbridges are much too large to exhibit Josephson-like behavior, and the junctions are actually

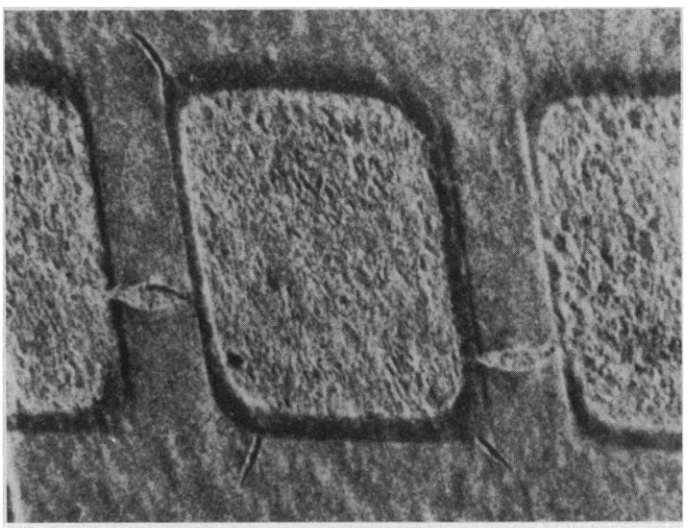

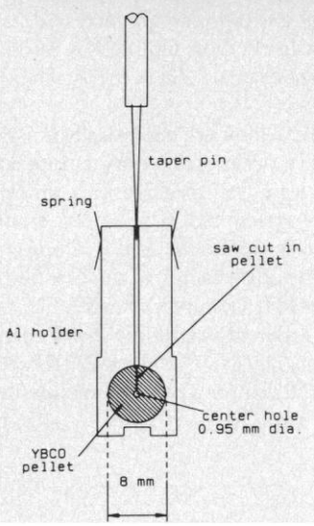

Fig. 6. (**Top**) The dc SQUID fabricated from thin-film of YBCO (*11*). The inside dimensions of the loop are 40 by 40 μm. (**Left**) The rf SQUID made from a pellet of YBCO (*40*).

formed by the grain boundaries between randomly oriented grains of YBCO. This patterning technique had the disadvantage of reducing the transition temperature of the protected regions for the relatively poor quality films available at the time. As the quality of the films improved, conventional patterning techniques such as lift-off (*36, 37*) and ion etching (*38*) have become possible without a concomitant reduction in the transition temperature or critical current of the patterned films. These SQUIDs exhibit hysteresis in the voltage when the applied flux is increased and then decreased to its original value, and the flux noise power scales approximately as $1/f$ over the range studied, typically 1 to 1000 Hz. The lowest noise energies in these SQUIDs to date (*39*) are 1.3×10^{-27} J/Hz at 1 Hz and 41 K and, in a different device, 4×10^{-26} J/Hz at 1 Hz and 77 K. These values are plotted in Fig. 4.

The most sensitive rf SQUID so far was reported by Zimmerman *et al.* (*40*). A hole was drilled along the axis of a cylindrical pellet of YBCO, and a slot cut part way along a radius (Fig. 6, left). The pellet was glued into an aluminum holder and the assembly immersed in liquid N_2. A taper pin forced into the slot in the mount caused the YBCO to break in the region of the cut; when the pin was withdrawn slightly, the YBCO surfaces on the two sides of the crack were brought together forming a "break junction." The rf SQUID so formed was coupled to a resonant circuit and operated in the usual way. The best magnetic flux resolution was $4.5 \times 10^{-4}\ \Phi_0$

$Hz^{-1/2}$ at 50 Hz, corresponding to a noise energy of 1.6×10^{-27} J/Hz for $L = 0.25$ nH (Fig. 4).

Flux Noise in YBCO Films

It is apparent that the $1/f$ noise level in YBCO SQUIDs is extremely high. To investigate the source of this noise, Ferrari *et al.* (*41*) measured the flux noise in YBCO films. Each film, deposited on a $SrTiO_3$ chip, was patterned into a loop and mounted close to a Nb-based SQUID (with no input coil) so that any flux noise in the YBCO loop could be detected by the SQUID. The assembly was enclosed in a vacuum can immersed in liquid ^{4}He. The SQUID was maintained at 4.2 K, while the temperature of the YBCO film could be varied. Below T_c, the flux-generated flux noise had a spectral density that scaled as $1/f$ over the observed range of 1 to 10^3 Hz, and increased markedly with temperature. Three films were studied, with their microstructure progressively improved with respect to the fraction of grains oriented with the *c*-axis perpendicular to the substrate. The critical current density correspondingly increased, to a value of 2×10^6 A cm^{-2} at 4.2 K in the best film. It was found that the low-frequency noise decreased dramatically as the quality of the films was improved.

These results demonstrate that YBCO films are intrinsically noisy: the noise is believed to arise from the motion of flux quanta trapped in the film, possibly at grain boundaries. This mechanism is almost certainly the origin of the $1/f$ noise observed in SQUIDs made from YBCO. It is encouraging that the noise can be reduced by improving the microstructure of the films: the noise energy in the best film, with an estimated inductance of 400 *p*H, was approximately 10^{-27} J/Hz at 1 Hz and 77 K, a value an order of magnitude lower than that observed in the dc SQUIDs, and 7×10^{-29} J/Hz at 27 K (see Fig. 4). Thus, low-noise SQUIDs will require very high quality or possibly single-crystal films. Although such films are now becoming available, their lack of grain boundaries implies that alternative means of making junctions will have to be found, for example, normal-metal bridges. Furthermore, the noise induced by an input coil or flux transformer coupled to the SQUID may be considerable, so that these components should also be of very high quality films.

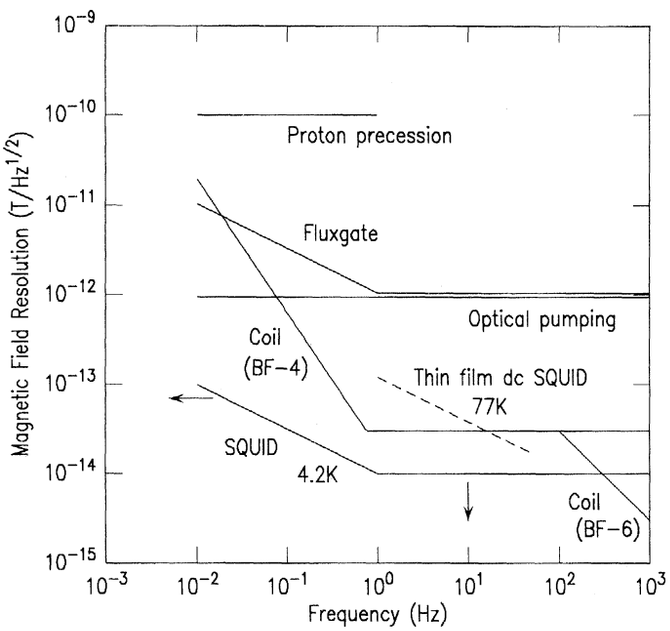

Fig. 7. Performance of various magnetometers. The coils are manufactured by Electromagnetic Instruments, Inc.; the noise for the other nonsuperconducting instruments is intended to be representative. The white noise of the 4.2 K SQUID magnetometer has been arbitrarily chosen to be 10^{-14} T/Hz$^{1/2}$; higher sensitivities and lower $1/f$ noise have both been achieved (indicated by arrows). The predicted performance of the 77 K SQUID as a magnetometer (dashed line) assumes an ideal, noise-free flux transformer with a 50-mm diameter pick-up loop.

High T_c Magnetometers

We now assess the prospects for magnetometers involving high T_c SQUIDs. This is not an entirely straightforward task, since the performance of the SQUIDs is still evolving, and it is clear from the experiments on YBCO films that thin-film flux transformers may introduce substantial levels of low-frequency noise. Because high T_c superconducting wire is not yet available, the question of its noise properties hardly arises. To make progress we simply use the results for the lowest noise reported in a dc SQUID at 77 K and assume it can be optimally coupled to a noiseless flux transformer with a pick-up loop radius of 25 mm. The resulting sensitivity is shown in Fig. 7. We note that although the noise energy at 1 Hz of a dc SQUID at 77 K is about five orders of magnitude higher than that of a typical dc SQUID at 4.2 K, the magnetic field resolutions shown in Fig. 7 differ by only one order of magnitude. This difference arises partly because $B_z(f)$ scales as $\varepsilon^{1/2}(f)$ (see Eq. 4) and partly because we have used a bigger pick-up loop for the high T_c magnetometer. As the quality of films used in high T_c SQUIDs is improved, the intrinsic low-frequency noise will undoubtedly be reduced, with a corresponding improvement in the sensitivity of magnetometers, providing the noise contribution of the flux transformer can be made negligible.

Nonsuperconducting Magnetometers

For comparison with the SQUID-based instruments, we briefly review the performance of four magnetometers (*42*) that operate at room temperature. Representative sensitivities are plotted in Fig. 7. The noise levels of a variety of fluxgate magnetometers (*43*) which, like SQUID magnetometers, are vector instruments have been reviewed by Primdahl (*44*). The most sensitive instruments have a noise level as low as 1×10^{-12} T/Hz$^{1/2}$ at 1 Hz with a spectral density scaling as $1/f$ at lower frequencies. The frequency response typically extends to about 1 kHz. The proton precession magnetometer (*42*) measures the absolute value of the ambient field. The resolution of the best instruments is typically 10^{-10} T for a 1-Hz sampling rate. Since each sampling process involves only the measurement of a frequency, the drift rate is very low. Optically pumped magnetometers (*42*) also measure the total field from the shift it induces in the atomic energy levels of an alkali metal vapor or ^{4}He. Under optimum conditions, one can achieve a resolution of 10^{-12} T/Hz$^{1/2}$. In airborne surveying of local variations in the earth's magnetic field, two spatially separated magnetometers can be used as a gradiometer.

Induction coils, which are widely used for magnetotellurics and controlled-source electromagnetic sounding, produce a voltage in response to a time-varying magnetic flux. Coils can be used at frequencies as high as 10^5 Hz and as low as 10^{-3} Hz, the frequency range covered depending on the number of turns, which can vary from a few thousand to 25,000 or more. The output of the coil is connected to an amplifier that at low frequencies inevitably exhibits $1/f$ noise. Because the voltage response of the coil falls off as f, the spectral density of the magnetic field noise scales as $1/f^3$ at low frequencies. The noise above 1 Hz can be remarkably low, however,

typically 3×10^{-11} T/Hz$^{1/2}$. In coils specifically designed for higher frequency operation, the noise can be less than 1×10^{-14} T/Hz$^{1/2}$ at frequencies extending from a few hundred hertz to tens of kilohertz (*45*).

Looking at Fig. 7, we see that liquid-^{4}He SQUID magnetometers are more sensitive than any other magnetometer, particularly at frequencies below ~1 Hz, with the possible exception of coils above about 100 Hz. One should bear in mind, of course, that one could improve the sensitivity of the SQUID magnetometers by increasing the size of the pick-up loop. The predicted noise in the high T_c SQUID magnetometer, which assumes a noiseless flux transformer, is below that of the fluxgate, proton precession, and optically pumped magnetometers, but higher than that of coils at least from about 0.1 Hz to 10 Hz. We emphasize that a high T_c magnetometer with this sensitivity has not yet been built. Thus, for the near future, coils are likely to remain the instruments of choice for geophysical applications such as magnetotellurics and electromagnetic sounding.

Concluding Remarks

Considering the short time that has elapsed since the discovery of high T_c superconductors, SQUIDs based on these materials have made remarkable progress. However, they have not yet developed to the point where they are likely to have a major impact as measuring instruments. For most applications, the increase in the white noise in the dc SQUID as the temperature is increased from 4.2 K to 77 K is not too significant. In the case of the rf SQUID, the white noise should be relatively unaffected as the temperature is increased from 4.2 K to 77 K. On the other hand, because most applications of SQUIDs are at low frequencies, the high levels of $1/f$ noise at 77 K are very serious, and must be greatly reduced if a useful instrument is to be produced. One may reasonably hope that in the foreseeable future the $1/f$ noise will be reduced sufficiently to enable one to use SQUIDs in such applications as geophysics, where the required sensitivity is not too high. In this case, the use of liquid N_2, which has a latent heat of vaporization about 60 times higher than liquid ^{4}He, would enable one to operate a cryostat unattended in the field for long periods—up to about a year. Operation of SQUIDs in liquid Ne with a boiling point of about 28 K and a latent heat roughly 40 times that of ^{4}He might offer a significantly improved noise performance over that at 77 K, with only a small reduction in the running time. Alternatively, one might consider rather small, easily portable cryostats filled with liquid N_2 or Ne that could be used in remote areas for several weeks without replenishment.

The situation is different, however, for the more demanding applications such as neuromagnetism. Here, one needs very high sensitivity, but is not particularly concerned with the cost of liquid ^{4}He or the need to replenish it at frequent intervals. Furthermore, low-noise, closed-cycle refrigerators are just becoming available that obviate the need to supply liquid cryogens in environments where electrical power is available. Thus the development of instruments for neuromagnetism is unlikely to be influenced by high T_c SQUIDs unless there is a major breakthrough in performance.

Two key problems must be solved before high T_c SQUIDs are likely to be technologically important. The first concerns the development of a reproducible and reliable Josephson junction. A junction with an insulating barrier like that in Fig. 1, top, would represent an enormous technological breakthrough, but the high-temperature processing necessary for these ceramic materials makes this a formidable problem. Perhaps superconductor–normal metal–superconductor junctions or bridges offer greater hope. An Anderson-Dayem bridge is another alternative, but the extremely small dimensions required make the fabrication extremely difficult. The second problem is concerned with the reduction of magnetic field hysteresis and noise in thin films of high T_c material. The motion of magnetic flux in the films is responsible for both effects, and one has to learn how to produce films in which the concentration of flux lines is greatly reduced or the flux is much more strongly pinned. Possibly materials other than YBCO will be better in this regard.

Thus, the development of high T_c SQUIDs into useful devices will involve considerable progress in materials science. Given the world-wide effort on the new superconductors, there is every reason to be optimistic about the future of SQUIDs and other high T_c devices, and to expect they will play a significant role in future electronics.

REFERENCES AND NOTES

1. See, for example, J. Clarke, *Phys. Today* **39**, 36 (1986); *IEEE Trans. Electron Devices* **ED-27**, 1986 (1980).
2. B. S. Deaver and W. M. Fairbank, *Phys. Rev. Lett.* 7, 43 (1961); R. Doll and M. Näbauer, *ibid.*, p. 51.
3. B. D. Josephson, *Phys. Lett.* **1**, 251 (1962).
4. J. G. Bednorz and K. A. Müller, *Z. Phys.* **B64**, 189 (1986).
5. M. K. Wu *et al.*, *Phys. Rev. Lett.* **58**, 908 (1987).
6. H. Maeda *et al.*, *Jpn. J. Appl. Phys.* **27**, L209 (1988), part 2.
7. Z. Z. Sheng and A. M. Hermann, *Nature* **332**, 138 (1988).
8. W. C. Stewart, *Appl. Phys. Lett.* **12**, 277 (1968).
9. D. E. McCumber, *J. Appl. Phys.* **39**, 3113 (1968).
10. P. W. Anderson and A. H. Dayem, *Phys. Rev. Lett.* **13**, 195 (1964).
11. R. H. Koch *et al.*, *Appl. Phys. Lett.* **51**, 200 (1987).
12. P. Chaudhari *et al.*, *Phys. Rev. Lett.* **60**, 1653 (1988).
13. R. C. Jaklevic, J. Lambe, A. H. Silver, J. E. Mercereau, *ibid.* **12**, 159 (1964).
14. F. C. Wellstood, C. Heiden, J. Clarke, *Rev. Sci. Instrum.* **55**, 952 (1984).
15. M. B. Ketchen and J. M. Jaycox, *Appl. Phys. Lett.* **40**, 736 (1982).
16. J. M. Rowell, M. Gurvitch, J. Geerk, *Phys. Rev. B* **24**, 2278 (1981).
17. C. D. Tesche and J. Clarke, *J. Low Temp. Phys.* **29**, 301 (1977).
18. R. H. Koch, D. J. Van Harlingen, J. Clarke, *Appl. Phys. Lett.* **38**, 380 (1981).
19. C. T. Rogers and R. A. Buhrman, *Phys. Rev. Lett.* **53**, 1272 (1984); R. H. Koch, in *Noise in Physical Systems*, M. Savelli, G. Leroy, J. P. Nougier, Eds. (North-Holland, New York, 1983), pp. 377–380.
20. A. van der Ziel, *Physica* **16**, 359 (1950).
21. Biomagnetic Technologies, Inc., 4174 Sorrento Valley Boulevard, San Diego, CA 92121.
22. R. H. Koch *et al.*, *Low Temp. Phys.* **51**, 207 (1983).
23. V. Foglietti *et al.*, *Appl. Phys. Lett.* **49**, 1393 (1986).
24. C. D. Tesche *et al.*, in *Proceedings of the 17th International Conference on Low Temperature Physics*, U. Eckern, A. Schmid, W. Weber, H. Wuhl, Eds. (North-Holland, New York, 1984), pp. 263–264.
25. F. C. Wellstood, C. Urbina, J. Clarke, *Appl. Phys. Lett.* **50**, 772 (1987).
26. J. E. Zimmerman, P. Thiene, J. J. Harding, *J. Appl. Phys.* **41**, 1572 (1970).
27. CTF Systems, Inc., 15-1750 McLean Avenue, Port Coquitlam, British Columbia, Canada V3C 1M9.
28. J. Kurkijärvi, *Phys. Rev. B* 6, 832 (1972).
29. ——— and W. W. Webb, in *Proceedings of the Applied Superconductivity Conference*, H. M. Long and W. F. Gauster, Eds. (IEEE, Piscataway, NY, 1972), pp. 581–587.
30. J. Clarke, in *Superconductor Applications: SQUIDs and Machines*, B. B. Schwartz and S. Foner, Eds. (Plenum, New York, 1976), pp. 67–124.
31. In making these estimates, we use the formula $L_p = \mu_0 r_p[\ln(8r_p/r_0) - 2]$ for the inductance of the pick-up loop, where r_0 is the radius of the wire. For a reasonable range of values of r_p/r_0, we approximate this expression by $L_p = 5\mu_0 r_p$.
32. For a review, see G. L. Romani *et al.*, *Rev. Sci. Instrum.* **53**, 1815 (1982); D. S. Buchanan *et al.*, *Adv. Cryo. Eng.*, in press.
33. C. D. Tesche, L. Krusin-Elbaum, W. D. Knowles, *Brain Res.*, in press.
34. J. Knuutila, M. Kajola, R. Mutikainen, J. Salmi, in *Extended abstracts for the 1987 International Superconductivity Electronics Conference*, Tokyo, 28 and 29 August 1987 (The Japanese Society of Applied Physics, Tokyo, 1987), pp. 261–264.
35. P. Carelli and V. Foglietti, *J. Appl. Phys.* **54**, 6065 (1983).
36. P. K. Mankiewich *et al.*, *Appl. Phys. Lett.* **51**, 1753 (1987).
37. B. Häuser, M. Diegel, H. Rogalla, *ibid.* **52**, 844 (1988).
38. R. H. Koch *et al.*, *Physica C* **153–155**, 1685 (1988).
39. R. L. Sandstrom *et al.*, *Appl. Phys. Lett.* **53**, 444 (1988).
40. J. E. Zimmerman, J. A. Beall, M. W. Cromar, R. H. Ono, *ibid.* **51**, 617 (1987).
41. M. J. Ferrari *et al.*, *ibid.* **53**, 695 (1988).
42. For a review, see W. F. Stuart, *Rep. Prog. Phys.* **35**, 803 (1972).
43. D. I. Gordon, *IEEE Trans. Magn.* **MAG-8**, 76 (1972).
44. F. Primdahl, *J. Phys. E* **12**, 241 (1979).
45. Electromagnetic Instruments, Inc., P.O. Box 463, El Cerrito, CA 94530.

46. We are grateful to A. Becker, D. Crum, R. Kleinberg, E. A. Nichols, R. E. Sager, H. Siegel, M. B. Simmonds, and G. Tibensky for helpful discussions on nonsuperconducting magnetometers. We thank R. L. Fagaly and J. E. Zimmerman for supplying Figs. 3 (top) and 6 (left), respectively. This work was supported in part by the Director, Office of Energy Research, Office of Basic Energy Sciences, Materials Sciences Division of the U.S. Department of Energy under contract No. DE-AC03-76SF00098 and the Office of Naval Research.